Welding in the World (2023) 67:1313–1324
https://doi.org/10.1007/s40194-022-01461-8

RESEARCH PAPER

Application of nickel plating by galvanization on steel surface of brazed cemented carbide-maraging steel joints

W. Tillmann[1] · T. Ulitzka[1] · L. Dahl[2] · L. Wojarski[1] · H. Ulitzka[1] · M. Koymatli[1]

Received: 1 September 2022 / Accepted: 28 December 2022 / Published online: 26 January 2023

Abstract

Recently, the integration of a maraging steel heat treatment into a vacuum brazing has been conducted successfully to manufacture high-strength and sound cemented carbide-steel joints with elevated mechanical properties of the steel component. Besides the use of low-melting silver-based active filler alloys and cost-intensive palladium-containing filler alloys, the application of a nickel layer on the maraging steel surface by an arc-PVD process is an adequate approach to overcome the low wettability of those steels, which is caused by high fractions of elements with a high oxygen affinity like titanium and molybdenum. Though nickel plating by arc-PVD is an elaborate and time-consuming coating process, it is not suitable for industrial applications since a high vacuum is required in the specimen chamber and only a small number of specimens can be processed at the same time.

Therefore, this publication evaluates the application of nickel galvanization by chemical plating and electroplating as an alternative nickel-coating method to manufacture a brazed joint between a cemented carbide and maraging steel (1.2709) component by using the copper filler metal Cu 110 (T_M = 1085 °C). The electroplated and PVD-coated reference specimens featured a sound joint from a minimum nickel layer thickness of 7.0 µm with a similar microstructure consisting mainly of a copper-based fillet and a nickel-rich phase band at the maraging steel-fillet interface. The chemical-plated specimens showed excessive diffusion between the joining partners due to the presence of melting point depressant phosphor between 10.5 and 12.0 wt.-% in the applied characteristic nickel-phosphorus layer. Consequently, titanium migration occurred from the maraging steel surface to the cemented carbide-fillet interface, and columnar iron-cobalt phases formed originating from the cemented carbide into the copper-rich fillet. Except for the specimens coated with no nickel and a 2.5-µm PVD layer, all brazed joints featured a shear strength of at least 150.0 MPa. The maximum shear strength of 344.8 MPa was achieved by electroplating the maraging steel joining surface with a 20.0-µm-thick nickel layer. Moreover, the steel heat treatment was carried out successfully since an elevated and homogenous hardness of at least 648 HV1 was measured in all steel specimens after brazing.

Keywords Vacuum brazing · Cemented carbide · Heat treatment · Maraging steel · Microstructure · Joint strength · Galvanization · Wetting

1 Introduction

Brazed tools with a cemented carbide-steel joint, like machining inserts, milling cutters, or tool holders, require a combination of a high joint quality (e.g., high joint strength and sound joint) and elevated mechanical properties of the steel components [1]. Good mechanical properties of the steel component in terms of increased strength, toughness, and hardness values are required to ensure that the tools retain their shape during cutting and do not wear abrasively due to numerous tool changes on the clamping surfaces. This way, workpieces can be manufactured with high tolerances,

Recommended for publication by Commission XVII - Brazing, Soldering and Diffusion Bonding

✉ T. Ulitzka
tim.ulitzka@tu-dortmund.de

[1] Institute of Materials Engineering, TU Dortmund University, Dortmund, Westphalia, North Rhine, Germany

[2] Sandvik Coromant, Stockholm, Sweden

and in the interests of sustainability, tools with a long service life can be produced [2].

Industrially, brazing is widely used and established as a joining process to manufacture high-quality and durable cemented carbide-steel tools [3]. In the application, one or more abrasion-resistant cemented carbide tips with a comparatively small volume are usually induction brazed to an already machined and heat-treated tool steel carrier under an argon atmosphere. In brazing processes with a local heat input, such as laser and induction brazing, carbon-hardening tool steels will experience the formation of an unrelaxed martensite in the direct vicinity of the brazing zone as a result of exceeding the austenitizing temperature, and the process-related high cooling rates after the brazing process, which is also referred to as glass hardness [4, 5] in the literature. This undesirable microstructural transformation of the steel component is disadvantageous for several reasons. The already high residual stresses in the joint, critical for the joint quality, are superimposed by additional stresses resulting from the volume increase due to martensite formation. The phase boundary between the unannealed martensite and the softened steel structure is referred to as a metallurgical notch [4].

In contrast to brazing processes with local heat input, heat input during brazing in a furnace under high vacuum with or without argon partial pressure occurs comprehensively and comparatively slowly due to the prevailing heat transfer modes [6]. Due to the process, all components in the furnace and, thus, also the steel carrier material are exposed to the temperatures occurring during the brazing process. Accordingly, proper heat treatment of the steel component before the brazing process to set the mechanical target values is not expedient since the microstructure and the mechanical properties of the steel component are negatively affected by the elevated temperatures and the low cooling rates required for carbide-steel brazes [2].

Recent publications have shown that by integrating a heat treatment of a maraging steel into the vacuum brazing process for carbide-steel joints, a combination of high joint quality and correspondingly high mechanical values of the steel component could be achieved [1, 7]. Unifying these otherwise contrasting directions was made possible by exploiting the hardening mechanism of such maraging steels, whose martensite formation is independent of the cooling rate from the solution annealing temperature [8]. Wetting of maraging steels by conventional metallic brazing materials is difficult due to the oxygen affinity of titanium, aluminum, and chromium alloying elements by conventional brazing materials [9]. Suitable brazing systems like gold-based brazing alloys [10, 11], palladium-alloyed brazing alloys [10–12], and titanium-containing active alloys [7, 11] or a coating of the joining surface with, e.g., nickel [10, 11], can ensure wetting by metallic brazing materials and consequently improve the strength of the brazed joint.

The use of active filler metals [7] and the coating of the maraging steel surface with nickel by the arc-PVD process [1] are two approaches used to produce high-quality carbide-steel joints by vacuum brazing. The use of electroplating to coat with nickel has been used in the past to produce similar types of maraging steel brazed joints [10]. However, a transfer of this coating method for manufacturing cemented carbide-maraging steel brazed joints has not been documented yet.

2 Materials

2.1 Cemented carbide (EMT 210)

As a joining partner for the steel, the cemented carbide grade EMT 210 with a grain size of ~ 0.8 µm was used. The chemical composition is displayed in Table 1. For the brazing tests, the EMT 210 was used as a cylinder (Ø = 10 mm, h = 5 mm). The EMT 210 cylinders were machined from a round bar by an electrical discharge machining (EDM) process and subsequently ground (600 pp) to free the joining surface from organics and oxide layers.

2.2 Braze material

Pure copper was used for the brazing tests in the shape of a foil with a thickness of 100.0 µm (Table 2). The melting temperature of pure copper is 1083 °C, and the recommended brazing temperature is 1100 °C. This brazing temperature is significantly higher than the recommended solution annealing interval of the maraging steel 1.2709. In contrast to silver-based filler metal systems, pure copper features a complete solubility with the coating element nickel [14]. Copper-solid solutions experience an improvement in mechanical properties with increasing nickel content. Thus, copper was selected as a filler material to investigate the possibility of alloying the brazing fillet during the brazing process.

Table 1 Chemical composition of cemented carbide in wt.-% (supplier: Extramet) [13]

WC	Co	Additional carbides
89.0	10.0	1.0

Table 2 Chemical composition of used braze materials in wt.-% with corresponding process temperatures (supplier: Wesgo)

	Cu	T_S	T_L	T_B	t_F
Unit	wt.-%	°C	°C	°C	µm
	100.0	1085	1085	1100	100

2.3 Maraging steel 1.2709 (X3NiCoMoTi18-9–5)

As a joining partner for the cemented carbide component, the maraging steel grade 1.2709 was used (Table 3). The 1.2709 is a low-carbon tool steel with a regular solution annealing temperature between 810 and 900 °C and a dwell time between 10 min and 1 h [15, 16]. It features a bulk hardness of ca. 350 HV1 in the soft-annealed state and reaches a maximum of ca. 600 HV1 when tempered at 490 °C for at least 3 h. For the brazing tests, the round bars were machined into the shape of a cylinder (Ø = 20 mm, h = 5 mm). The steel cylinders were finely ground (1200 pp) on one side to free the joining surface from organics and oxide layers. All joining materials were cleaned in ethanol by ultra-sonic bath for 5 min before being positioned in the vacuum furnace chamber.

3 Experimental procedures

3.1 PVD deposition of nickel coating

The maraging steel joining partners, except the benchmark brazements, were coated with PVD nickel layers of varying thicknesses. Therefore, the joining surface was first ground (1200 pp) and polished with a diamond suspension (1 µm). Subsequently, the specimens were nickel-plated in a Metplas 20'' vacuum arc evaporator using a nickel cathode. Primarily, the joining surfaces were ion etched under vacuum ($p = 3 \times 10^{-4}$ mbar, 100 A, − 1000 V bias voltage, 3 Ah) to free it from organics and oxide layers and other contaminations and to avoid the formation of new oxide layers. Subsequently, the steel samples were coated with nickel layers with thicknesses of 0 (0 Ah, 90 A, 30 V), 2.5 (30 Ah, 90 A, 30 V), 7.5 (90 Ah, 90 A, 30 V), and 10 µm (120 Ah, 90 A, 30 V).

3.2 Specimen geometry and shear testing

The cemented carbide cylinder and the punched brazing foil (Ø = 12 mm, h = 100 µm) were positioned centrally on the maraging steel cylinder before being placed in the furnace chamber (Fig. 1, upper right corner). The samples were assembled and shear tested using a shear device set-up to assess the joint strength properties, as previously conducted in [1]. A steel cylinder is positioned in the gap of the shear strength test device and, therefore, can only be moved in the loading direction. The notch, which was eroded into the surface of the device, holds the joining partners in the correct position and guarantees an evenly distributed force transfer into the brazing seam along with the profile of the cemented carbide cylinder. The applied force was constantly raised with a rate of 1 kN/s until the braze joint failed and the cemented carbide cylinder sheared off. The ultimate shear strength was then calculated by the quotient of the maximum measured force and the initial joining surface (A = 78.5 mm^2). The solidified brazing fillet outside the brazing seam was not removed before determining the shear strength of the braze joint. A statistically validated mean value for the shear strength was generated using the arithmetic mean of three shear samples per batch.

3.3 Nickel plating by galvanization

3.3.1 Nickel electroplating

The maraging steel joining surface was electroplated by an external company. Since it is not possible for the company to precisely set the coating thickness given the small coating quantity, the coating is carried out using experience process values. Achieved coating thicknesses were measured afterwards using X-ray. Since maraging steel forms stable oxide layers, the samples were first coated with nickel-strike. The coating surface was ground and polished, as was the case with the PVD-coated specimens,

Table 3 Chemical composition of used steel grades in wt.-% (supplier: Abrams Premium Stahl) [15]

Steel	Fe	C	Mo	Ni	Co	Ti
1.2709	Bal.	< 0.03	5.00	18.00	10.00	1.00

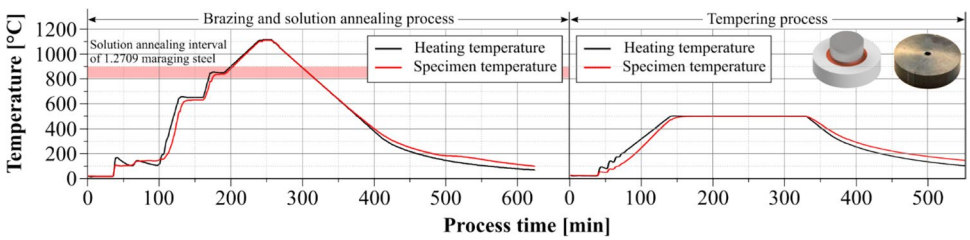

Fig. 1 Time–temperature profile of the brazing respectively solution annealing process (left) and tempering process (right) with brazing geometry and a dummy for temperature regulation (upper right corner)

before applying the nickel-strike electrolyte. Nickel-strike is an electrolyte usually used to conduct a pre-treatment on difficult-to-coat surfaces like stainless steel or already nickel-plated surfaces. The nickel-strike electrolyte breaks the stable oxide layers on the substrate and thus supplies ideal coating conditions. Applied nickel-strike coatings have a pure nickel-coating thickness of ca. 1 µm. Nickel-strike coatings are performed at room temperature (pH < 0). As displayed in Table 4, one experiment is conducted only by applying a 1.0-µm-thick nickel layer by nickel-strike. The remaining samples were then electroplated at 60 °C (pH = 4.4). The achieved total coating thicknesses were 7.0 and 20.0 µm.

3.3.2 Nickel-chemical plating

The same external company carried out the chemical coatings. Again, a nickel-strike layer was applied first, and the chemical coating was carried out subsequently. The chemical coating was carried out at a temperature of 90 °C (pH = 4.8). The phosphorus content of the chemical coating generally amounts between 10.5 and 12.0 wt-%. It is important to note that phosphorus lowers the melting temperature of the nickel-phosphorus layer system to about 870–890 °C [17]. Thus, the applied layer will melt even before the brazing temperature of 1100 °C is achieved. The used chemical-plated nickel-phosphorus layer thicknesses were estimated based on the exposure time and process experience. The reached layer thicknesses were set up to 5.0 and 10.0 µm. An overview of all sample batches is shown in Table 4. In the following, the coating classification refers to the last coating step. Therefore, e.g., a nickel-phosphorus coating (10.0 µm) with a previously applied Ni strike (10.0 µm) is referred to as "10.0 µm Ni–P."

3.4 Brazing process and steel heat treatment

As previously described and suggested in [1] and [7], an integration of a maraging steel heat treatment into a vacuum brazing process of cemented carbide-steel joints leads to a combination of good joint properties with a shear strength of at least 150 MPa and a sound joint as well as elevated mechanical properties of the steel component. The vacuum brazing process, respectively, solution annealing process, for the 1.2709 is displayed in Fig. 1 (left). The first 100 min of the brazing process was dedicated to the realization of a high-quality vacuum since a vacuum-sensitive active filler alloy was used. A heating rate of 20 °C/min was set up to a temperature of 650 °C. At 650 °C, a heating plateau was initiated for 15 min, and argon partial pressure of 10^{-1} mbar was introduced to the furnace chamber to avoid copper evaporation. A second heating plateau was established at 850 °C for 10 min. From 850 °C, the specimens were heated up with a decreased heating rate of 5 °C/min to the brazing temperature of 1100 °C for 10 min to guarantee a homogenous heat distribution within the joining partners. Here, heating temperature means the actual temperature of the heating elements measured with a thermocouple reaching into the furnace chamber with a distance of 10.0 mm to the right-sided heating element. Here, the brazing temperature of 1100 °C is 200 °C higher than the recommended solution annealing temperature of the 1.2709. Preliminary tests showed that the increase in solution annealing temperature due to the elevated brazing temperature of the copper filler material (T_{Br} = 1100 °C) did not negatively impact the hardening mechanism. After the dwell time of 10 min, a regulated cooling phase with a rate of 5 °C/min was initiated to a temperature of 300 °C to keep the residual joint stresses at a minimum. From 300 °C, the specimens were further cooled down to room temperature by vacuum cooling. The tempering temperature of 490 °C was selected based on the tempering diagram of the 1.2709 and held for 3 h (Fig. 2, right) to obtain maximum strength and hardness values for the maraging steel component. A dummy made of the maraging steel grade 1.2709 (d = 20.0 mm, h = 5.0 mm) was used for temperature regulation. The thermocouple was put in a previously drilled hole of 1.5 mm in diameter and 2.5 mm in depth in the center of the dummy (Fig. 1, upper right corner).

3.5 Wetting test

The wetting of the substrate by the molten filler metal is an essential property in the field of brazing, especially when a good wettability is required to fill wide and long gaps. Besides the wetting angle, the spreading ratio S is a qualitative measurement approach and usually used to describe the wettability of a molten filler metal on a

Table 4 Coating variations of maraging steel joining surface

Coating process	Sample batches		
[-]	Uncoated		
PVD	2.5 µm Ni coating	7.5 µm Ni coating	10.0 µm Ni coating
Nickel-strike	Ni-strike (1.0 µm Ni coating)		
Electroplating	Ni-strike + 7.5 µm Ni coating		Ni-strike + 20.0 µm Ni coating
Chemical plating	Ni-strike + 5.0 µm Ni–P coating		Ni-strike + 10.0 µm Ni–P coating

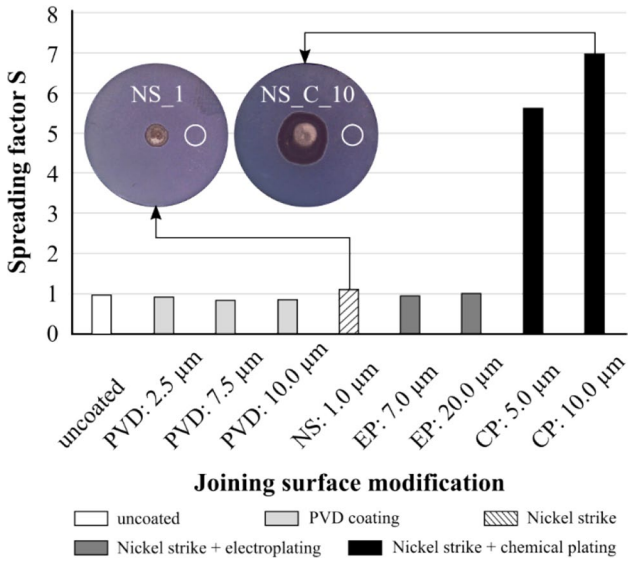

Fig. 2 Spreading factor of Cu110 on different maraging steel surface coatings with NS, nickel-strike; EP, electroplating; and CP, chemical plating

specific substrate [18]. The spreading ratio S is defined as $S = A_f/A_s$, where A_f is the covered area by the molten and solidified filler metal after brazing and A_s is the default area of the solid brazing foil before the brazing process. In this study, a round element with a diameter of $d_L = 3$ mm is punched out of the present copper foil with a thickness of 100.0 µm (Table 2) using a mechanical hand punch. Therefore, the default area can be calculated to $A_s = 7.1$ mm^2. The default area is displayed as a white circle in Fig. 2. The wetted area A_f was then subsequently measured with a Leica "DVM6" digital microscope. The wetting tests were carried out on a 1.2709 maraging steel cylinder with a diameter of 20.0 mm and a height of 5.0 mm, whereas the steel surface was either previously ground (1200 pp) or non-treated after the respective coating method.

3.6 Hardness indentation

The measured hardness values were determined by a Vickers hardness tester (Struers, Duramin 40) on a cross section of the cemented carbide-steel joints applying a load of 1 kgf (kilogram-force) and a loading time of 15 s. A pattern of 18 indents (3 × 6 indents) evenly distributed over the cross section of the steel part was applied. The approach of hardness testing is further documented in [19]. By evenly distributing over the whole cross section is herein meant that the indents should be placed so that they cover the entire cross section with a slight variation in the distance between them according to DIN EN ISO 6507.

3.7 Light optical microscopy

The prepared cross sections were examined under the Olympus BX51M light optical microscope. In each case, overview images of the entire brazed seam were taken. The light microscopic images allow different phases to be better distinguished.

3.8 SEM/EDS analysis

The SEM–EDS technique was used to analyze the microstructure of the brazed joint and the base materials. The SEM used was a Jeol JSM-7001F using high-resolution field emission scanning electron microscopy (FE-SEM) with a thermal field emission cathode (Schottky). The mentioned SEM was used to investigate the joint microstructure and crack propagation and to determine the chemical composition of the occurring phases by EDS.

4 Results and discussion

4.1 Wetting behavior

The spreading factor was determined for each maraging steel joining surface modification to investigate the wetting behavior. The spreading factor of each layer type is shown in Fig. 2. The spreading ratio S was almost independent of the nickel coating in case pure nickel was applied. It ranged around $S = 1$ for all coating with pure nickel, specifically between 0.86 (7.5-µm PVD coating) and 1.12 (1.0-µm nickel-strike). The uncoated specimen in this context featured a spreading factor of $S = 1.14$. Only the chemical nickel-phosphorus coating led to a significant increase in the spreading factor. At a coating thickness of 5.0 µm, approximately a fivefold increase, and for a layer thickness of 10.0 µm, a sevenfold increase in the spreading factor compared to the spreading factor of the uncoated reference sample was determined. The influence of phosphorus in the coating seems to be decisive. As described in the prior part, the high proportion of phosphorus with 10.5–12.0 wt-% leads to a significant decrease in the melting temperature of the coated layer to about 870–890 °C. Thus, the layer melts even before the melting temperature of the filler metal with a melting temperature of 1083 °C is reached. The molten nickel-phosphorus alloy solves the brazing material during the heating phase right before the brazing step. A diffusion of phosphorus from the nickel layer into solid copper-based filler material is also possible, reducing its melting point and consequently lowering the viscosity of the melt. An additional explanation for the excessive flow of the copper braze on the applied nickel-phosphorus layer might be reasoned in the deoxidizing effect of phosphorous. Phosphorus

is generally used as a deoxidizing agent to produce oxygen-free copper. In the brazing industry, phosphorus is used as a melting point depressant in nickel- and copper-based filler metals to braze difficult to wet stainless steels and copper alloys [20–22]. It is assumed that the phosphorus inhibits the formation of further oxides within the copper filler during the brazing process, thus increasing the displayed flowing properties.

4.2 Microstructure analysis and crack propagation

4.2.1 Microstructure and crack propagation of PVD-coated specimens

Figure 3 gives an overview of the brazed joint conducted with the maraging steel 1.2709, featuring no joining surface coating and different PVD nickel thicknesses ranging from 2.5 to 10.0 µm. An improved bonding with increasing nickel layer thickness can be observed when comparing the different microstructures. In the case of no applied nickel coating, a continuous crack was observed at the interface between the maraging steel and the copper-based fillet (Fig. 3, column 1). Despite the occurring crack, a strong interaction between the molten filler and the maraging steel was detected since the copper-based fillet has infiltrated the maraging steel, preferably at the grain boundaries of the steel. The infiltration took place to such an extent that parts of the maraging steel base material were detached and moved into the brazing seam. In this context, copper diffusion into the grain boundaries of the steel can eventually lower the mechanical properties of the steel at the described interface by causing a loss of ductility, which in literature is also referred to as liquid metal embrittlement [23]. Despite the signs of a strong fillet-based material interaction at the steel-filler interface, no sound joint was realized. This bad connection at the fillet-steel interface can be attributed to the high fractions of elements with a high oxygen affinity. The continuous crack occurs as a result of an insufficient bonding and serves in the following as the crack propagation path. The cross-section analysis of the failed joint reveals, without exception, a crack propagation at the maraging steel-filler interface. Only small red phases can be detected at the edge of the maraging steel, originating from the previous base material infiltration.

Applying a 2.5-µm-thick PVD nickel layer on the maraging steel results in a better bonding between the copper-based fillet and the maraging steel (Fig. 3, column 2). A less severe crack with a lower crack width is still visible at the maraging steel-fillet interface. Also, the crack is partially interrupted by a firm bond between the copper-based fillet and the maraging steel surface. When comparing the specimen with a 2.5-µm nickel coating (Fig. 3, column 2) to the one without a nickel coating (Fig. 3, column 1), the extent of infiltration of the base material is reduced. The crack propagation is still occurring at the maraging steel-fillet interface but is shifted a few micrometers into the copper fillet. The brazements of the maraging steel with a 7.5- (Fig. 3, column 3) and 10.0-µm-thick PVD nickel layer (Fig. 3, column 4) featured a sound joint. Whereas the brazement with the 7.5-µm nickel layer, if at all, features very few nanoscale defects, the brazement with the 10.0-µm nickel coating shows no defects. Between the copper-based fillet (spectrum 1 in Table 5) and the maraging steel (spectrum 3 in Table 5), a third nickel-rich phase occurred (spectrum 2 in Table 5). This nickel-rich phase is mainly enriched in nickel (65.2 wt.-%) originating from the pre-applied PVD nickel layer. But it also features relatively high amounts of iron (20.2 wt.-%) and copper (10.4 wt.-%), which indicates the diffusion of elements from the filler material and the steel

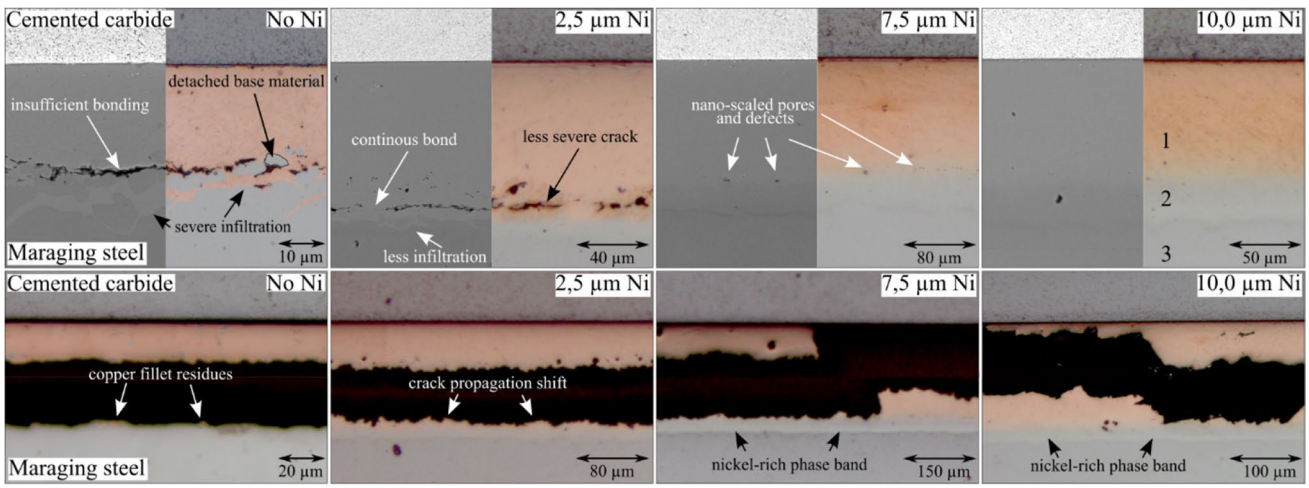

Fig. 3 Cross sections (first row) with SEM image (left) and light microscope image (right) and crack propagation (second row) of brazements without nickel coating and varying PVD-nickel layer thicknesses

Table 5 Chemical composition of the measuring points in Fig. 3 in wt.-%

Spot/element	Fe	Co	Ni	Cu	Ti
1	0.5	3.5	4.0	92.0	-
2	20.2	3.6	65.2	10.4	0.6
3	68.6	10.6	19.9	-	0.9

base material. Just like elements from the filler material and the filler metal diffuse into this layer, other elements diffuse in the opposite direction. Consequently, nickel was detected in the copper-based filler metal (4.0 wt.-%) as well as in the base material with a higher amount (19.9 wt.-%) than the chemical composition of the maraging steel would suggest (18.0 wt.-% Ni in Table 3).

The 7.5- and 10.0-µm-thick nickel layers serve as a diffusion barrier for the copper-based filler metal. No copper penetration of the grain boundaries of the maraging steel, as it was the case with no nickel coating, was detected. Another indicator that the applied nickel layer serves as a diffusion layer is reasoned in the decreased migration of iron from the steel to the cemented carbide-fillet interface. As known for cemented carbide-steel joints brazed with copper and documented in [24], iron diffuses through the copper fillet, which has a very limited iron solubility. As a result, the iron precipitates together with the cobalt originating from the cemented carbide as columnar γ-Fe-Co phases growing from the cemented carbide into the copper-rich fillet. The formation of such columnar γ-Fe-Co phases can eventually lead to the embrittlement of the cemented carbide component by cobalt binder depletion and η-carbide formation. Compared to the specimens with no nickel coating and a 2.5-µm PVD nickel coating, the crack propagates at the interface between the copper-based fillet and the nickel-rich phase, through the copper fillet and along the cemented carbide-fillet interface.

Furthermore, the applied PVD nickel layer is responsible for the molten filler remaining in the brazing gap. The oxide layer of the uncoated specimen restricts diffusion between the fillet and the steel, resulting in a more severe wetting of the cemented carbide component. Therefore, the copper-based molten filler metal is pushed out of the brazing gap, covering the cemented carbide cylinder even at the side. Consequently, the brazing gap of the uncoated specimen ranges between 30.0 and 40.0 µm (Fig. 3, column 1), which is a reduction of more than half compared to the default thickness of the pure copper foil of 100.0 µm. The coated specimens all feature wider brazing gaps after the brazing process. While the specimen with a 2.5-µm nickel coating features a brazing gap of around 60 µm (Fig. 3, column 2), the final brazing gap of the specimens with a 7.5- and 10.0-µm nickel coating (Fig. 3, columns 3 and 4) was in the range of the copper foil thickness. An increased diffusion between the molten filler metal and the base material, as well as an increased viscosity or even isothermal solidification of the molten filler metal as a result of nickel migration from the applied layer, might be responsible for the significantly wider brazing gaps.

4.2.2 Microstructure and crack propagation of electroplated specimens

The microstructure of the cemented carbide-maraging steel brazement with a 20.0-µm-thick nickel coating applied by electroplating is represented in Fig. 4 since it shows the highest shear strength values of all specimens. When analyzing the microstructures, it becomes evident that the microstructures of the electroplated and PVD-coated samples are similar in their respective phase formation. As known from the samples with a 7.5- and 10.0-µm coating, a nickel-rich phase has formed between the copper-rich fillet and the maraging steel. All diffused elements dissolve in the copper matrix. Increasing the thickness of the nickel layer also leads to improved bonding in these samples. However, it must be noted that no thin, electroplated nickel layer was investigated, and a comparison with the specimen with a 2.5-µm nickel coating was not possible. Therefore, no infiltration of the maraging steel by the molten filler can be detected (Fig. 4, left), as it is the case with the PVD-coated specimens with an increased coating thickness. With an increase in the

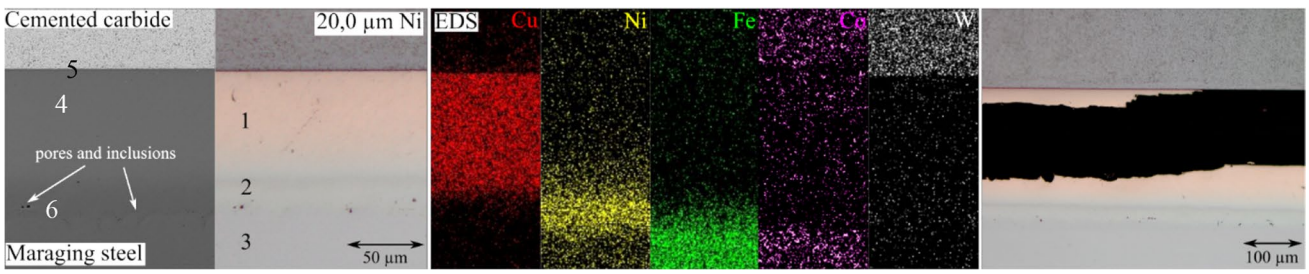

Fig. 4 Cross sections (SEM and light microscope image, left), EDS mapping (mid), and crack propagation (right) of brazements with 20-µm nickel coating conducted by electroplating

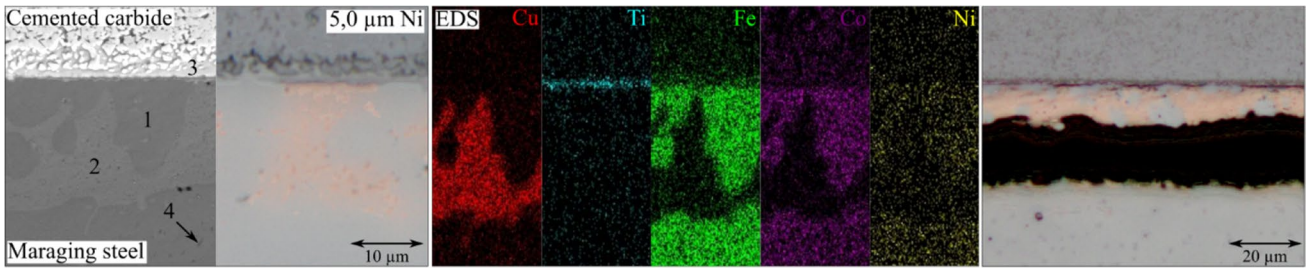

Fig. 5 Brazed joint microstructure of specimen coated with 5.0- (left) and 10.0-µm (right) nickel-phosphorus layer

layer thickness, a decrease in pores and cracks in the joint can be observed. In the case of the specimen with a 20.0-µm nickel coating, no cracks and only a few pores can be detected, which indicates a better oxide layer removal of the ion etching during the PVD process compared to the application of the nickel-strike electrolyte (Fig. 4, left).

The EDS scan in Fig. 4, mid, shows the distribution of the elements within the brazing seam. The fillet mainly consists of a copper phase (red) with small element fractions of nickel (4.7 wt.-%) and cobalt (2.8 wt.-%). Also, the nickel-rich phase band is visible (spectrum 2 in Table 6) between the copper-rich fillet (spectrum 1) and the maraging steel base material (spectrum 3). The EDS mapping of the brazed joint indicates a nickel accumulation where the nickel layer was previously applied by electroplating. A decreasing gradient into the fillet and the maraging steel indicates nickel diffusion. The measured chemical compositions of the nickel-rich phase and the base material (Table 6) are similar to the ones measured for the brazement using a specimen with a 10.0-µm nickel coating (Table 5). Furthermore, an increase in nickel content was measured at the interface between the cemented carbide and the fillet (spectrum 5 with 2.4 wt.-% Ni), even though almost no nickel was measured in the direct vicinity of the interface in the copper-based fillet (spectrum 4). The nickel migrates through the molten filler during the brazing process and precipitates at the cemented carbide-fillet interface. The precipitation at this interface strengthens the interface as cemented carbides are nickel-plated [25] for that reason. When analyzing the crack propagation, the crack mainly propagates through the copper-based fillet. The general overview of the crack propagation, which is not shown here due to lack of space, shows a strongly fissured copper fillet (Fig. 4, right). The high strength values of the joint, as well as the propagation through the fissured copper-based phase, which is generally known for its high ductility, indicate an increased ductility compared to the brazements with a lower nickel-coating thickness, which failed with almost no deformation. Between the filler-steel interface, rod-shaped titanium-sulfur phases have formed (spectrum 6 in Table 6) due to the sulfur introduced by the electroplating process. These phases might be possible for the occurrence of pores between the steel and the nickel-rich phase band [26].

4.2.3 Microstructure and crack propagation of chemical-plated specimens

The cross sections of the brazed joints of the specimens with a chemical nickel-phosphorus layer featured a different phase formation in the brazing seam (Fig. 5, left). When observing the joint, a significant part of the filler metal was squeezed out of the brazing seam. The braze gap thickness is only 10.0 to 20.0 µm wide. The braze gap thicknesses of the samples with a pure nickel layer (PVD and electroplating) showed significantly wider brazing gaps between 60.0 and 95.0 µm. The bonding in the chemically coated samples is deteriorated by pores and bonding defects (Fig. 6). The pores are assumably caused by remaining oxides on the maraging steel surface and the outgassing of phosphorus from the nickel-phosphorus layer. When examining the

Table 6 Chemical composition of the measuring points in Fig. 4 in wt.-%

Spot/element	Fe	Co	Ni	Cu	Ti	S
1	-	2.8	4.7	92.5	-	-
2	31.5	4.7	63.3	0.1	0.4	-
3	65.7	11.0	22.4	-	0.9	-
4	0.2	3.2	0.3	-	96.3	-
5	-	2.2	2.4	95.4	-	-
6	42.4	7.6	24.8	-	16.7	8.5

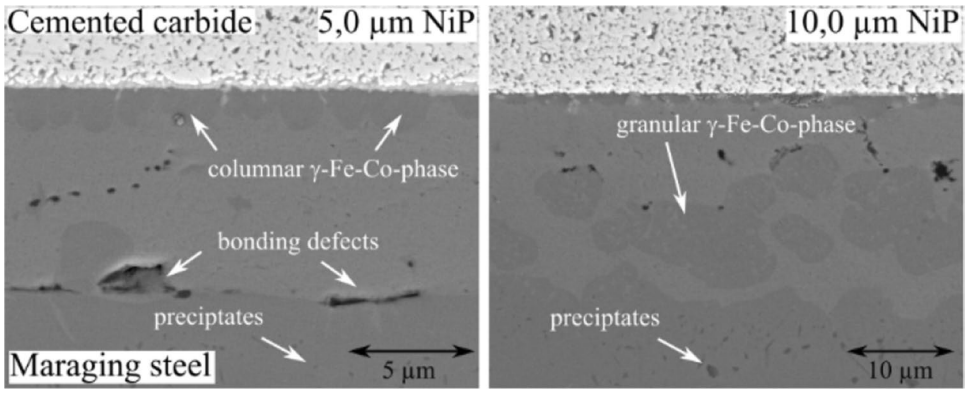

Fig. 6 Cross sections (SEM and light microscope image, left), EDS mapping (mid), and crack propagation (right) of brazements with 5.0-µm nickel coating conducted by chemical plating

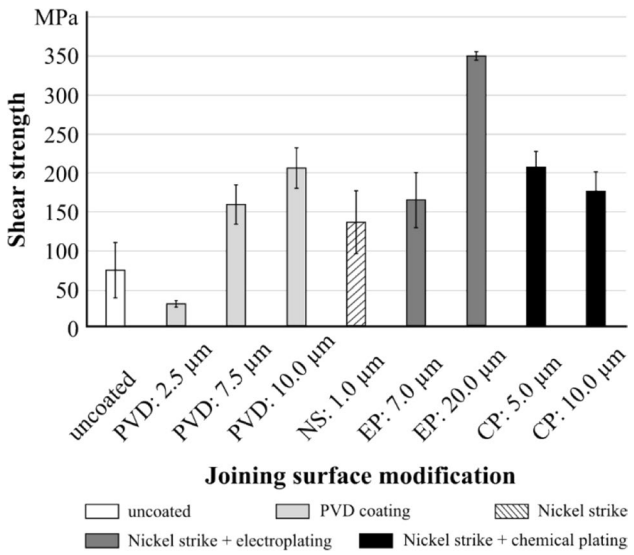

Fig. 7 Shear strength values of brazed joints depending on maraging steel coating with NS, nickel-strike; EP, electroplating; and CP, chemical plating

microstructure of the samples coated with a 5.0-µm-thick nickel-phosphorus layer, it becomes evident that a new phase formed during the brazing process. Chemical analysis with EDS showed the formation of γ-Fe-Co phases (Fig. 5, left and spectrum 1 in Table 7), which are also documented in the literature [24]. These columnar γ-Fe-Co phases growing into the copper-based fillet can also be identified by EDS mapping (green, purple, and yellow in Fig. 5, mid). When comparing the specimens with a 5.0- and a 10.0-µm nickel-phosphorus coating, it is noticeable that the microstructure of the γ-Fe-Co phase changes (Fig. 6). For the specimen with the 5.0-µm-thick nickel-phosphorus layer, the γ-Fe-Co phase grows from the cemented carbide-fillet interface in a columnar manner towards the maraging steel into the copper-rich fillet (Fig. 6, left), in some cases even reaching through the whole brazing seam (Fig. 5, left, light microscope image). In contrast, the specimen with the 10.0-µm-thick nickel-phosphorus layer, the γ-Fe-Co phases are centrally present in the brazing seam in a granular shape (Fig. 6, right). Also, a finer and dispersed phase of the same chemical composition was detected within the copper-based brazing seam. The formation of a titanium layer at the cemented carbide interface is visible in both coating thicknesses (cyan, EDS mapping in Fig. 5). Due to the low titanium content of 1.0 wt.-% in the maraging steel, this is surprising. Because titanium is only present in the maraging steel, it must have migrated through the molten filler metal to the cemented carbide-fillet interface, eventually forming a titanium carbide, as it is known for active brazing of cemented carbides [7]. This could subsequently lead to embrittlement of the brazed seam. However, this assumption cannot be sustained based on the present test results. Although no significant amount of phosphorus originating from the applied nickel-phosphorus layer was detected in the brazing seam by mapping, small, elongated phosphorus-containing precipitations were detected in the steel base material close to the fillet-steel interface (spectrum 4 in Fig. 5 and Table 7). The titanium content in these phases is also strongly increased (17.9 wt.-%). Grain boundary penetration of the steel with copper is visible to a severe extent in both

Table 7 Chemical composition of the measuring points in Fig. 5 in wt.-%

Spot/element	Fe	Co	Ni	Cu	Ti	W	P
1	38.1	34.2	10.3	17.2	-	-	-
2	8.8	5.5	3.8	81.9	-	-	-
3	7.4	8.7	1.2	2.6	0.5	79.6	-
4	36.7	14.5	11.1	2.6	17.9	-	17.2

coating thicknesses since γ-Fe-Co phases can be found in the fillet (spectrum 1 in Fig. 5, left). When observing the crack propagation for both layer thicknesses, the crack propagation runs along the boundaries of the γ-Fe-Co phases at the fillet-maraging steel interface (Fig. 5, right).

4.3 Shear strength analysis

Figure 7 shows the arithmetic mean and the standard deviation of the shear strength values of the conducted brazing tests varying the maraging steel joining surface modification. As shown in Fig. 7, considerable differences become apparent. The shear strength values of the specimens with a nickel coating, generally with shear strength values over 150 MPa, were significantly higher than those without a nickel coating ($\sigma_{Shear} = 70.1 \pm 34.0$ MPa). Only the PVD-coated sample with a thin layer thickness of 2.5 µm led to lower shear strength values ($\sigma_{Shear} = 26.8 \pm 4.2$ MPa). When pure nickel is plated (PVD or electroplating), a higher plating thickness leads to higher joint shear strengths. The highest shear strength was detected by applying the electroplated layer with a thickness of 20.0 µm ($\sigma_{Shear} = 344.8 \pm 12.1$ MPa). Here, the shear strength is almost five times higher than the one of the specimens without a coating. When comparing the shear strengths of a 7.5-µm-thick nickel layer applied by PVD ($\sigma_{Shear} = 154.6 \pm 24.8$ MPa) to a 7.0-µm-thick one used by electroplating ($\sigma_{Shear} = 162.2 \pm 35.4$ MPa), both coating processes result in similar shear strengths values. Since both coating processes led to a very similar element diffusion and phase formation in the brazing seam (Figs. 3 and 4), similar mechanical behavior in response to the shear load is reasonable. In this context, the coating process seems to have a subordinate influence on the brazing result.

Specimens chemically coated with a nickel-phosphorus layer also resulted in high shear strength values over 150.0 MPa. An increase in nickel-phosphorus layer thickness from 5.0 µm ($\sigma_{Shear} = 201.7 \pm 21.7$ MPa) to 10.0 µm ($\sigma_{Shear} = 170.7 \pm 25.2$ MPa) resulted in a decrease in shear strength (Fig. 7). When analyzing the brazed joint microstructure, both coating thicknesses led to the formation of distinct γ-Fe-Co phases, but with different morphology and position inside the brazing seam (Fig. 6). There is disagreement in the literature about whether the formation of γ-Fe-Co phases leads to an increase or decrease in strength ([1, 27, 28]). Based on the present results, it can be assumed that the influence of the microstructure of the γ-Fe-Co phases is significant.

4.4 Hardness tests

The hardness tests on the steel component were carried out to verify whether the integrated heat treatment process led to the desired hardening of the maraging steel. Similar high hardness values were achieved for all sample batches, with slight variations probably resulting from the different positions in the furnace chamber and consequently a slight difference in heat distribution. For all steel specimens, the mean hardness ranged between 648.8 and 660.5 HV1, where the lowest measured value was 646.1 HV1, and the highest value was 668.5 HV1. The standard deviation ranged between 2.7 and 5.7 HV1. The characteristic values obtained by the described hardness analysis of the specimen coated with a 7.0-µm-thick nickel coating by electroplating are displayed in Table 8. According to the data sheet, the maximal achievable hardness is around 600 HV when properly heat treated between 820 and 850 °C for 1 h and tempered at 490 °C for 6 h, whereby the applied load during hardness indentation was not specified. Based on the acquired data, the hardening of the 1.2709 was carried out to the full extent.

5 Conclusion and outlook

This paper investigated the influence of surface modification of the maraging steel joining surface by different nickel coatings for cemented carbide-steel joints. For this purpose, the joining partners made of maraging steel were coated by PVD and electroplating and chemical plating. Furthermore, the influence of different coating thicknesses with respect to joint microstructure, shear strength, and wetting behavior was investigated. In addition, it was investigated whether the heat treatment integrated into the brazing process led to a sufficient hardening of the maraging steel. The most important discoveries are summarized below:

1) Applying a pure nickel layer (PVD and electroplating) on the maraging steel led to a higher quality of the brazed joint. The application with pure nickel with a minimum thickness of 7.0 µm significantly improved the bonding. It thus increased the shear strength of the brazed joint, whereby the increase in layer thickness positively influenced the brazing seam. The average shear strength was increased from 70.1 (uncoated specimen) to 344.8 MPa (20.0 µm nickel layer by electroplating). Moreover, at higher coating thicknesses, sound joints were found.

Table 8 Exemplary hardness analysis in HV1 for the electro-plated specimen with a nickel layer thickness of 7.0 µm

Modification	Mean value	Minimum value	Maximum value	Standard deviation
EP: 7.0 µm	651.1	646.4	657.2	3.1

2) The application of a nickel-phosphorus layer also led to a significant increase in shear strength. For the specimens with a 5.0 nickel coating, an average shear strength of 201.7 MPa was achieved. However, an increase in the nickel-phosphorus layer thickness led to a decrease in the shear strength.
   a. The chemically coated nickel-phosphorus layer led to a greatly improved wetting and excessive flow of the copper-based filler metal. In addition, the presence of phosphorous in the brazing seam resulted in an excessive increase in diffusion processes. As a result, an interlayer of titanium formed at the fillet-cemented carbide interface.
   b. A γ-Fe-Co phase formed for both coating thicknesses, but with different morphology and position.
3) Integrating the maraging steel heat treatment into the brazing process led to a significant increase in the hardness of the maraging steel. The maraging steel had a hardness of more than 648 HV1 for all brazing processes.

In further studies, a more extensive variation of the coating thickness would be interesting. In this study, the highest shear strength increase was achieved with the thickest nickel layer thickness of 20.0 µm. An even further increase in nickel coating thickness with respect to phase formation, joint strength, and wetting behavior was not investigated yet. Small-step experimental investigations to find an optimum layer thickness range could benefit industrial processes since no PVD is required anymore. Furthermore, more detailed studies of brazing with a nickel-phosphorus layer are promising. Since the phosphorus lowers the melting temperature of the layer to 870–890 °C, it could be possible to braze with pure copper as a filler metal below the melting [29], which is 1085 °C. On the one hand, this could reduce the thermally induced residual stress of the joint as well as the grain growth of the steel component, which leads to an embrittlement of the steel component [30]. On the other hand, the reduction in brazing temperature will have economic and ecological benefits since process times can be reduced.

Funding Open Access funding enabled and organized by Projekt DEAL.

Data Availability The datasets generated during and/or analysed during the current study are available from the corresponding author on reasonable request.

Declarations

Conflict of interest The authors declare no competing interests.

References

1. Tillmann W, Ulitzka T, Dahl L, Wojarski L, Ulitzka H (2022) An investigation of the influence of integration of steel heat treatment and brazing process on the microstructure and performance of vacuum-brazed cemented carbide/steel joints. Weld World 66:1053–1066. https://doi.org/10.1007/s40194-022-01266-9
2. Tillmann W, Ulitzka T, Dahl L, Wojarski L (2021) A novel approach to manufacture long-lasting, wear-resistant tools. In: International Brazing and Soldering Conference – IBSC 2021, Denver
3. Schimpfermann M, Schnee D (2015) Brazing in the tool manufacturing industry. Saxonia, Hanau, pp 1–38
4. Stahlhut C (2011) Laserstrahllöten von Stahl und Hartmetall für zerspanende Werkzeuge mit definierter Schneide. Gottfried Wilhelm-Leibniz-Universität Hannover, Hannover
5. Schimpfermann M, Wiehl G, Rassbach S, Magin M, Kazuch A, Marchi M, Unnasch N (2019) Fundamental study on tempered state of steel influenced by the brazing process parameters for joining of hard metal saw teeth to steel saw blades. In: Brazing, high temperature brazing and diffusion bonding - LÖT 2019, Aachen, pp 32–39
6. Peter HJ (2008) Induktionslöten - eine bewährte Fügetechnologie mit innovativem Zukunftspotential. In: Schweißen und Schneiden, vol 60, pp 216–221
7. Tillmann W, Ulitzka T, Dahl L, Salmanibideskan A, Wojarski L, Ulitzka H (2022) Potential of maraging steel as a joining partner for cemented carbide. In: Brazing, high temperature brazing and diffusion bonding - LÖT 2022, Aachen, pp 175–186
8. Davis JR (2001) Properties and selection: irons, steels and high-performance alloys. In: ASM handbook 1 ASM International, Materials Park, Ohio, pp 1–1063
9. Lang FH, Kenyon N (1971) Welding of maraging steels. In: WRC Bulletin, vol 159. New York, pp 1–41
10. Bradshaw JF, Sandefur PG, Young CP (1991) Braze alloy process and strength characterization studies for 18 nickel grade 200 maraging steel with application to wind tunnel models. NASA Langley Research Center, Hampton, United States, pp 1–52
11. Tillmann W, Wojarski L, Henning T (2019) The effect of nickel-plated surfaces on the microstructure and strength of vacuum brazed nickel maraging steel. In: Brazing, high temperature brazing and diffusion bonding - LÖT 2019, Aachen, pp 18–25
12. Berry RD (1965) Joining 18 per cent nickel maraging steels by brazing. In: Welding and metal fabrication, vol 3, pp 93–95
13. Extramet (2021) EMT 210 data sheet. https://www.extramet.ch. Accessed July 2022
14. Dies K (2014) Kupfer und Kupferlegierungen in der Technik. Springer, Publisher
15. Dörrenberg Edelstahl (2021) 1.2709 Data sheet: X3NiCoMoTi18–9–5. https://www.doerrenberg.de. Accessed: July 2022
16. Davis JR (2007) Heat treating. In: ASM handbook 4 ASM International, Materials Park, Ohio, pp 1–1012

17. Keong KG, Sha W (2002) Crystallisation and phase transformation behaviour of electroless nickel-phosphorus deposits and their engineering properties. Surf Eng 18(5):329–343
18. Persson U (2010) Iron-based brazing filler metals for high temperature brazing of stainless steel. In: Brazing, high temperature brazing and diffusion bonding - LÖT 2010, Aachen, pp 38–41
19. DIN EN ISO 6507-1 (2022) MetallischeWerkstoffe- Härteprüfung nach Vickers. DIN Deutsches Institut für Normung e. V, Berlin
20. Balart MJ, Patel JP, Gao F, Fan Z (2016) Grain refinement of deoxidized copper. Metall Mater Trans A, Elsevier 47:4988–5011
21. Dirnfeld SF, Gabbay R, Ramon JJ, Wagner HJ (1991) Copper embrittlement by silver brazing alloys. Mater Charact 26:17–22
22. Marsilius M, Hartmann T (2016) Influence of boron and phosphor containing nickel based brazing alloy on different base materials. In: Brazing, high temperature brazing and diffusion bonding - LÖT 2016, Aachen, pp 227–232
23. Kamdar MH (1983) Liquid metal embrittlement. Embrittlement Eng Alloys Elsevier 25:361–459
24. Ohmura H, Kawashiri K, Yoshida T (1988) Cemented tungsten carbide/carbon steel joint brazed with copper. Q J Japan Weld Soc 4:499–504
25. Zhu L, Luo L, Luo J, Wu Y, Li J (2012) Effect of electroless plating Ni–Cu–P layer on brazability of cemented carbide to steel. Surf Coat Technol 206:2521–2524
26. Riastuti R, Rifki A, Herdino F, Ramadini C, Siallagan ST (2018) Effect of saccharin as additive in nickel electroplating on SPCC steel. In: AIP Conference Proceedings, pp 1–6
27. Amelzadeh M, Mirsalehi SE (2019) Dissimilar vacuum brazing of cemented carbide to steel using double-layer filler metals. J Manuf Process 47:1–9
28. Weise W, Koschlig M, Herzog H et al (1998) Einsatz innovativer Lote in der Schneidtechnik. In: Brazing, high temperature brazing and diffusion welding, 5th International Conference, pp 62–67
29. Bazhenov VE, Pashkov IN, Pikunov MV (2013) Investigating crystallization processes while brazing copper by copper–phosphorus brazing alloy with the purpose of controlling the structure of the brased seam. Russ J Non-Ferrous Metals 54(1):43–47
30. Filho V, Barros I, Abreu H (2017) Influence of solution annealing on microstructure and mechanical properties of maraging 300 steel. In: Materials research 20, pp, 10–14